CHAPTER II

LITERATURE REVIEWS

This chapter has six major sections including a brief review of ceramic cutting tools, Al_2O_3-TiC composite, strengthening mechanism of Al_2O_3-TiC composite, fabrication of Al_2O_3-TiC, fundamental of combustion synthesis and, lastly, overview of microwave heating.

2.1 Ceramic Cutting Tools

The majority of cutting tools used in machining processes are made of cemented carbide and high-speed steel. However a variety of ceramic cutting tool materials was introduced in recent year and is now commercially used in a wide range of metal cutting application. Ceramic cutting tools can be used for turning cast iron and other metallic metal. In finishing operations, the only way to improve productivity is to increase cutting speed.

As seen in Fig. 2.1, since 1900, there has been an exponential increase in productivity capability as measured by cutting speeds available from ceramic cutting tools. The increasing in cutting speed produce higher cutting temperature, thus the mechanical properties of the cutting material at high temperature are obviously important. The ceramic cutting tool represents a different class of cutting tool materials with unique chemical and mechanical properties. In order to realize the full potential of ceramics, it is essential to have a clear understanding of all the variables which affect the performance of these tools. Variety types of cutting tool in Table 2.1 show composition for each type.

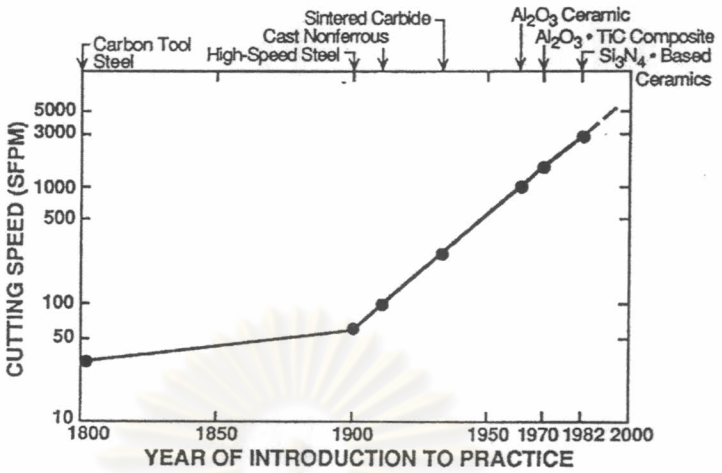

Fig 2.1 Improvements in cutting speeds for various cutting tools over time [9].

Table 2.1 Wide range of compositions for cutting tools.

Category	Compositions	Comments
Carbides	WC, SiC	Cemented carbides (WC) are sintered with metal. SiC-whisker reinforcements in ceramics.
Nitrides	BN, Sialon, TiN	BN is expensive because of high manufacturing cost. TiN is used as a coating for WC and high-speed steel.
Oxides	Alumina, Zirconia	Pure alumina has been replaced with alumina containing $\leq$ 15% of zirconia.
Carboxides	TiC dispersed in alumina	Called black ceramic, contained $\leq$ 40% of TiC to improve hardness.
Carbonitrides	TiN with carbide additions	Most commonly known as cermets because of metal binder phase.

Fig. 2.2 (a) illustrated the temperature dependence of strength for various type of cutting tools. Carbide has the highest bending strength at room temperature but the strength rapidly drops as the temperature rises up. The influence of the temperature on strength with cemented carbide and cermet is similar because both contain a metal phase as binder. Although silicon nitride and oxides have low strength at room temperature, their strengths exceed over 820^{o}C and remain constant to about 1100^{o}C [10].

Hardness is another critical property, it indicates wear resistance. Strengthening oxide ceramic by the addition of titanium carbide particle in alumina gives the higher hardness than pure oxide ceramics, as shown in Fig. 2.2 (b). Carboxide ceramic or Al_2O_3-TiC composite is typically containing 30 – 40wt%TiC. This material retains a higher hardness at high temperature than others tools and also more chemically inert. The combination of hot hardness and chemical inertness means that the Al_2O_3-TiC cutting tools can run at higher temperature and longer with less wear than the competing materials.

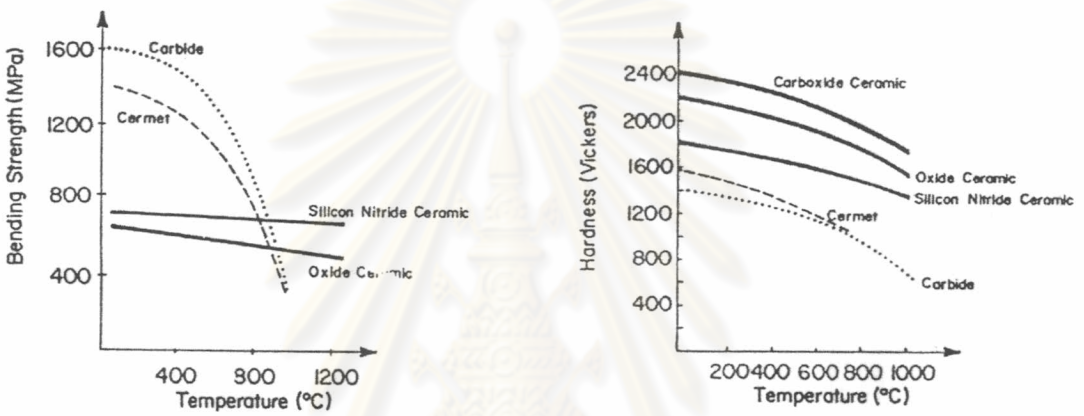

Fig. 2.2 (a) Hot strength and (b) hot hardness of cutting tool materials [10].

2.2 Al_2O_3-TiC Composite

Early generations of ceramic tools manufactured in the late 1940's and early 1950's were primarily cold pressed alumina. While these tools were chemically inert and had good hot hardness, they were notoriously low in toughness. This deficiency caused the tools to easily chip and break catastrophically, creating a poor image for early ceramic tools. The ceramic tools available today are consistent high quality, and when correctly applied, are capable of delivering a cost-effective performance on finish cuts of low hardness cast iron and medium hardness steels.

The development of the hot pressing process was a major step forward in producing high quality ceramic tools. This process allowed the addition of titanium carbide

particle to alumina, producing Al_2O_3-TiC composite, an excellent all proposes ceramic tool. This grade is available in a wide variety of standard insert configurations, which are shown in Fig2.3, at an affordable price (20-25% higher than coated carbides).

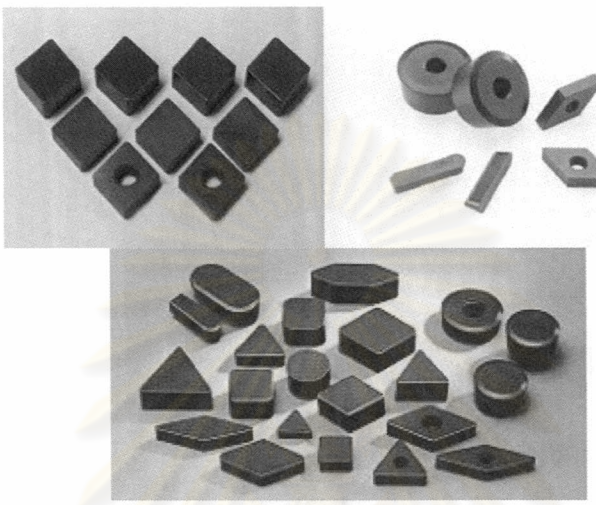

Fig. 2.3 A wide variety of standard insert configurations made from Al_2O_3-TiC composite.

Although other ceramic materials may be better for specific application, hot pressed Al_2O_3-TiC is acceptable for most machining situations where ceramics are applicable. It is an excellent material for turning tool steels as hard as 60-63 Rc, capable of holding diameters to a tolerance of $\pm$ 0.00025 inch and producing surface finish values of less than 5 micro-inch. This versatile ceramic material also has excellent thermal stability and is capable of cutting dry or with a water base fluid. The more relevant physical and mechanical properties of composite are shown in Table 2.2, in comparison with the values of pure alumina.

Table 2.2 Physical and mechanical properties of Al_2O_3 and Al_2O_3-TiC [11,12].

Materials	Density (g/cm^3)	Thermal expansion coefficient ($^oC^{-1}$)	Young's modulus (GPa)	Vikers hardness (HV0.5) (GPa)	Fracture toughness ($MPa.m^{1/2}$)	Four-point bending strength (MPa)		
						RT	700^{o}C	800^{o}C
Al_2O_3	3.98	8.01	396	18.70	3.24	436$\pm$35	346$\pm$35	364$\pm$19
Al_2O_3-TiC	4.38	7.94	410	20.71	4.27	785$\pm$86	565$\pm$52	495$\pm$122

It was obviously seen in Table 2.2 that alumina is strengthened by the addition of titanium carbide. The improvement of mechanical properties make this ceramic composite tool applicable for high speed machining and this facilitates the effective utilization of high-speed machines, reducing the machining time. The productivity is improved by shorter cycle time thus reduces the cost of manufacturing. Furthermore the lower thermal expansion coefficient can reduce thermal shock problem of pure alumina.

2.3 Strengthening Mechanisms of Al_2O_3-TiC Composite

Despite the fact that ceramics are inherently brittle, a variety of approaches have been used to enhance their fracture toughness and resistance to fracture. The essential idea behind all toughening mechanisms is to increase the energy needed to extend a crack. Simultaneously, the fracture toughness and bending strength of oxide ceramic are improved through crack deflection and crack bridging, caused by the dispersed hard particles as was shown in Fig.2.4. All of these mechanisms redistribute stress at the crack tip and increase the energy need to propagate a crack though the composite material, thereby resulting in improved toughening. The higher hardness in combination with the higher toughness increase the resistance to abrasive and erosive wear considerably.

(a) (b)

Fig. 2.4 Schematic of toughening mechanisms (a) crack deflection (b) crack bridging.

The Vickers hardness and fracture toughness of Al_2O_3-TiC were investigated by K.F.Cai et.al [13] as shown in Fig. 2.5. Both properties increase with increasing TiC volume fraction up to 30 vol% and can, almost certainly, be extrapolated to still higher values. Wahi an Ilshner [14] also found that the fracture toughness of hot-pressed Al_2O_3-TiC

composites increased with TiC content up to 35.1 vol%. The hardness of the composites increases gradually as TiC content increases; because TiC is relatively harder than Al_2O_3, while increasing fracture toughness is due to effects of crack deflection and crack bridging by TiC grain as shown in Fig 2.6. As the TiC content increases, the TiC grains or cluster become coarser, the more crack deflects and bridges.

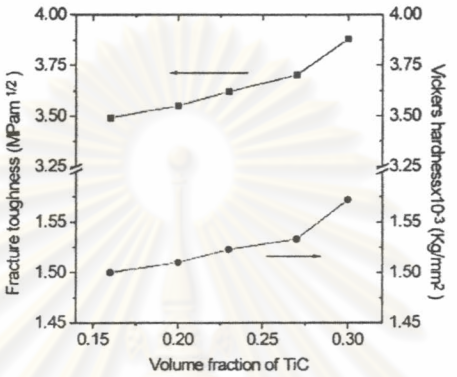

Fig.2.5 Fracture toughness and Vickers hardness as function of the volume fraction of TiC [13].

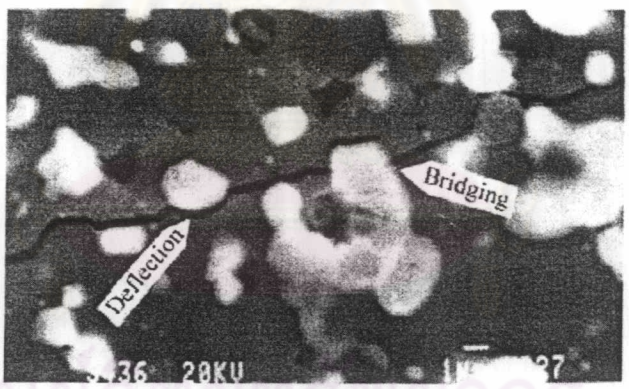

Fig. 2.6 Typical SEM micrograph of crack path of 16 vol%TiC sample induced by Vickers indentation [13].

It has been known that grain size is one of the most important factors that affect the mechanical properties of monolithic ceramic [15]. Y.Wan and J.Gong [16] evaluated the influence of the TiC particle size on the hardness of Al_2O_3-30%wt.TiC. It was found that the load-independent hardness increases with increasing TiC particle size as shown in Fig. 2.7. It is because of the lower linear coefficient of thermal expansion of TiC particle compared to that of Al_2O_3 matrix, $7.4x10^{-6}$ $^{\circ}C^{-1}$ and $8.8x10^{-6}$ $^{\circ}C^{-1}$ respectively [17],

thus residual stresses will develop in the Al_2O_3 upon cool down from sintering temperature. In the final products, the Al_2O_3 matrix would be placed in hoop tension and the TiC particles in radial compression. When an indentation is induced onto the surface of the test specimen, the newly formed free surface of the indentation, which encounters the interfaces between TiC particles and the Al_2O_3 matrix, would be partially subjected to radial compression, which may shorten the indentation diagonal and result in an increase in the material's hardness. Note that the magnitude of such residual internal stresses depend on the size of the TiC particle as well as the difference between the thermal expansion coefficient of the matrix and that of the particle. As a result, the hardness increases with the increasing TiC particle size.

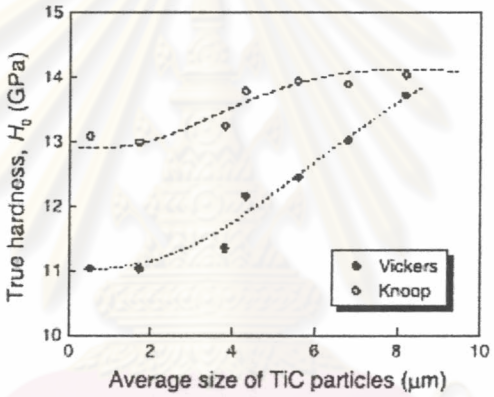

Fig. 2.7 Load-independent hardness number of Al_2O_3-30 wt%TiC composites as a function of average size of TiC particles in the test sample [16].

2.4 Fabrication of Al_2O_3-TiC Composites

Al_2O_3-TiC cutting tools have traditionally been made by either cold pressing followed with pressureless sintering or by hot-pressing. Powders with high purity and fine particle size were selected for the manufacturing. Uniform blending of these components is achieved through dry or wet milling. Organic binders are added to provide sufficient strength for performing process. The sintering process is very critical; the goal is to minimize porosity while maintaining a fine microstructure.

2.4.1 Pressureless Sintering

Comparing with hot-pressing and hot isostatic pressing, presureless sintering gives worse mechanical property material; however its production cost is lower. Therefore, preparation of Al_2O_3-TiC composites by presureless sintering has attracted attention and has been inspected [13,18]. Various additives were selected to prepare Al_2O_3-TiC composites, the propose was to lower the sintering temperature. Normally the sintering temperature of pressureless sintering was about 1800 – 1900 ^{o}C for 30 min. Aluminum 1wt.% additive was used in sintering at 1750 – 1800 ^{o}C for 30 min under an argon atmosphere in an induction furnace [13]. The relative density of samples were 97.5 -98.4 %TD, which indicated that using the aluminum additive can efficiently increase density.

An important problem that always inhibits fully densification of Al_2O_3-TiC composites is a gas-generating reaction between Al_2O_3 and either free carbon or combined carbon in TiC in pressureless sintering process. It has been reported by J.S.Choi et al. that this composite can be effectively densified by Y_2O_3 content additive at 1750^{o}C under an argon atmosphere [19]. This result was also confirmed by K.W.Chae et.al. [20]. The observed variation of the relative densities of sintered specimens with Y_2O_3 content is shown in Fig. 2.8. The density after sintering at 1600^{o}C was 92%TD and reached 97%TD after sintering at 1700^{o}C. The mechanism of Y_2O_3 suppressed gas generation was explained, however the amount of additive Y_2O_3 exceeds 0.35wt. % was not suggested because the density of specimens decreased and closed pores was not achieved.

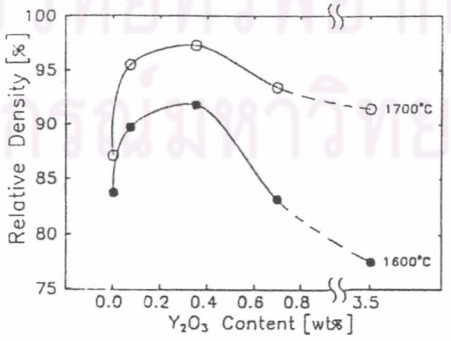

Fig. 2.8 The relative density of the Al_2O_3-30wt%TiC specimens as a function of the amount of Y_2O_3 [20].

2.4.2 Hot-Pressing

Hot-pressing or pressure sintering is a commonly used fabrication method that couples both thermal and mechanical energy to effect densification. Externally introduced compressions, the mechanical energy components, strongly influence the ceramic densification process. In general, the process is initiated by placing a powder mixture or precompacted form into a pressing cavity and then sintering by applying an appropriated time-temperature-pressure profile. The superimposed uniaxial load provides the mechanical energy and is usually applied simultaneously with heat during processing. The resultant increase in particle mobility and contact-stress within the powder or perform rapidly accelerates the kinetics of densification.

The advantages of the hot-pressing process relate directly to the additional energy source and the accompanying increased densification rate. Fully dense, fine-grained ceramic bodies can be fabricated at lower temperatures with shorter cycle times than those required by conventional sintering techniques, using equivalent starting powder parameter. Starting powder generally does not require large surface areas, and minimal amounts of sintering aids are needed. The disadvantages of the hot pressing are also related to producing the mechanical energy component. External pressure must be generated and, by definition, contained during processing. Therefore furnaces and associated equipment are costly when compared to pressureless sintering. The process is also limited in shape capability and is generally preformed on a batch basis.

Cutting tools have represented an outstanding commercial success for hot pressed ceramic [10]. One of the first commercially successful materials was a ceramic particulate composite of Al_2O_3-TiC [3]. Various conditions were used in previous studies, A.Tampieri et.al. obtained 99.5%TD of Al_2O_3-30 vol%TiC composite through hot-pressing at 1700 ^{o}C for 30 min. [11]. A using of lower temperature was found in others studies [16, 21,22], the Al_2O_3-TiC composites were prepared by hot-pressing carried out at 1650 - 1700^{o}C and 25 MPa for 30 min.

2.4.3 Hot-Isostatic Pressing

Recently, hot-isostatic pressing (HIP) has gained popularity as a manufacturing process for ceramics because improved equipment has become available. Several techniques have been developed for specific materials, but each tries to take advantage of the higher pressure available with HIP compared to hot-pressing.

Hot-isostatic pressing techniques can be divided into two categories: encapsulated and unencapsulated. In the unencapsulaed technique, previously sintered parts are heated in a furnace that is enclosed in a pressure vessel. A gas such as argon is pressurized to 100 to 300 MPa, and the combined heat and pressure remove any residual porosity left after the sintering step. For this technique, in order to the most effective, the starting density of the parts needs to be more than 93% to 95% of theoretical. This technique can be performed in a separate step after sintering, or, in the appropriately designed equipment, combined with sintering (sinter-HIP). Encapsulated technique consists of using a gas tight container to transmit the gas pressure to porous parts. Container materials always used high-temperature glasses or fused quartz.

HIP is thus a very versatile process with many advantages. In general, large voids in most materials can be efficiently reduced in size and frequency. Ceramic can be densified at relatively low temperature, including extremely difficult to sinter ceramics such as SiC, Al_2O_3-TiC, without any additive. The reduced sintering temperature means that grain growth and undesirable reaction can be controlled or avoided. A very high uniformity in properties can be obtained; an inherent feature of HIP is to produce parts with very accurate shape.

A comparison of HIP and hot-pressing Al_2O_3-TiC was study by S.J.Burden et.al. [3]. In both case, the microstructures were quite similar and the result of strength testing is shown in Table 2.3. The result of mechanical properties of hot-pressing product were higher than HIP because hot-pressing produces preferred orientation effect. It was proposed that the grains oriented perpendicularly to the hot pressed axis and interlocked in

a way that improved the strength in this plane. Although the measured mechanical properties of hot-pressed material were superior to the HIP material, the machining performance disagrees with strength data. Fig. 2.9 show the cutting test result, both tools gave inconsistent results; the average tool life was 36 min for HIP and 18.5 min for hot-pressed tools. All the tools failed by chipping except one HIP tool, the testing of which was stopped at 60 min. The strength produced by HIP was assumed to be equal in all direction; which play an important role in cutting performance.

Table 2.3 Mechanical properties of hot pressing and HIP Al_2O_3-TiC tool [3].

Material	MOR (MPa)		K_{IC} (MPa.$m^{1/2}$)
	at 20°C	at 1000°C	at 20°C
Hot-pressing	789 ± 94	598 ± 74	3.9 ± 0.1
HIP	673 ± 113	476 ± 43	3.4 ± 0.1

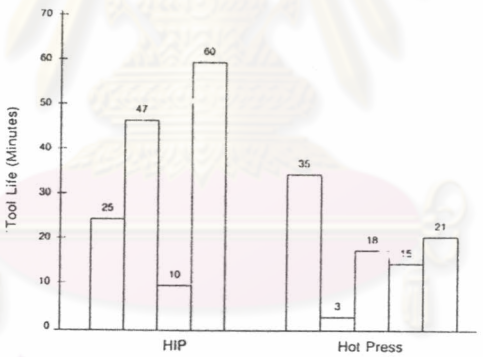

Fig.2.9 Tool life of Al_2O_3-TiC cutting tool turning A2 tool steel [3].

The major disadvantages, however, are the costs associated with equipment and the fact that the process does not lend itself to continuous production, since the pressing is carried out in an inert atmosphere.

2.4.4 Others fabrication

Al_2O_3-TiC composites can be produced by rapid rate sintering for pressureless sintering to avoid gas reaction as mentioned earlier [23, 24 and 25].

Furthermore, various additives were used for sintering aid such as TiO_2 [26] and Ti(Co) [27]. In addition, this composites are also fabricated by self-propagating high-temperature synthesis or SHS [28]; this process is gaining attention for synthesis materials and is therefore used to synthesize Al_2O_3-TiC powder in this research. More in-depth details of SHS will be discussed in the following section.

2.5 Self-Propagating High-Temperature Synthesis

The method that utilizes self-sustained exothermic reaction between reactants to prepare materials is called self-propagating high temperature synthesis (SHS) or combustion synthesis. This technique begins by initiating an exothermic reaction in an area of a reactant mixture, e.g. with a resistively heated tungsten wire. Once initiated, there is sufficient heat release that the reaction becomes self-propagating. This leads to the formation of a combustion wave which travels along the reactants, converting them to the required products [29].

2.5.1 Advantages of SHS Process

There are several advantages offered by SHS process as below.

2.5.1.1 Negligible energy requirement, simple and inexpensive equipment is sufficient for carrying out SHS process.

2.5.1.2 As very high temperatures are reached in reactions, all volatile impurities evaporate at these temperatures producing high-purity products.

2.5.1.3 The process can be used not only for producing powder but also to make near net shape components by utilizing the exothermic heat with processes such as casting, consolidation and coating.

2.5.1.4 The process offer high productivity as it has the highest reaction rates.

2.5.2 Theory of SHS Process

In general, SHS process is mass and energy transport limited. In these reactions energy is self generated. The maximum temperature or adiabatic temperature, T_{ad}, can be obtained from thermodynamic calculation as follow [30].

$$\Delta H^{r}_{To} = \int_{To}^{Tad} C_p dT \qquad (2.1)$$

where

ΔH^{r}_{To} = enthalpy of reaction at T_o

C_p = combined heat capacity of products

If the product constituents undergo any phase transformation below the T_{ad} thus calculated, then the corresponding changes in the enthalpy and heat capacities have to be taken into account and T_{ad} recalculated in a part-wise manner.

For instance, if one of the products is in the molten condition, then its melting point itself is the T_{ad} and the fraction in the molten condition, f, can be obtained from the equation,

$$\Delta H^{r}_{To} = \int_{To}^{Tm} C_p dT + f\Delta H_m \qquad (2.2)$$

where

ΔH_m = latent heat of fusion

T_m = melting point

In these calculation, it is assumed that all the heat generated by the reaction goes only to raise the temperature of the product and there is no loss of heat to the surrounding, meaning it is a closed system. Thus T_{ad} is only a measure of the exothermic reaction and defines the upper limit for any combustion system.

From the knowledge of the T_{ad}, certain system can either be eliminated for experimentation or combined with other more exothermic reaction to make them amenable

for SHS. Merzhanov has suggested an empirical criterion that if T_{ad} < 1500 K, combustion does not occur, and if T_{ad} ≥ 1800 K, the combustion reaction will become self-sustaining [4].

2.5.3 Experimental Parameters Affecting SHS Process

Several process variables affect the product quality and combustion velocity in SHS and these are discussed below.

2.5.3.1 Stoichiometric ratio: in general any deviation from stoichiometric ratio reduces the T_{ad}. Non-stoichiometric mixtures are sometime used to make up the loss of any species due to volatilization during combustion.

2.5.3.2 Sample diameter: the combustion rate increases with the specimen diameter and remains constant after reaching threshold value. This value depends on the combustion system.

2.5.3.3 Green density: thermal conductivity and specific heat of the green compact changes with the density of the compact. At low densities, the heat in the combustion front is not effectively transferred to the pre-combustion zone, and this can lead to oscillatory combustion or extinction of the reaction. Similar results are obtained at high densities due to rapid heat transfer from the combustion zone. An optimum density of the compact is desired to obtain steady state combustion.

2.5.3.4 Particle size: the effect of particle size on combustion has been examined earlier while discussing reaction mechanism. Several investigations show that propagation rates clearly increasing with decreasing particle size [31].

2.5.4 The Formation of Al_2O_3-TiC by SHS Process

SHS process has previously been used to produce Al_2O_3-TiC composites by a number of researches under the aluminothermic reaction as follow

$$3TiO_2 + 4Al + 3C \longrightarrow 3TiC + 2Al_2O_3 \qquad (2.3)$$

The adiabatic temperature can be used as a general indication of the temperature at the combustion front. It can also be used in a semi-quantitative way to ascertain whether the synthesis of a given materials can be accomplished by SHS method. It has been empirically suggested that combustion reaction will not become self-sustaining unless $T_{ad} \geq$ 1800 K. The theoretical adiabatic temperature of reaction (2.3) is 2330.98 K for rutile and 2331.27 K in the case of anatase; the calculation is shown in appendix A. Therefore, it can assume that the SHS reaction of equation (2.3) is possible from the preceeding theoretical results.

The sequential reaction mechanism to produce The Al_2O_3-TiC ceramic composites was studied by Y.Choi and S.W. Rhee [32]. Reaction a mechanism between each component investigared by Differential thermal analysis (DTA) was shown in Fig. 2.10. The stoichiometric coefficient represents the molar ratio of each component. While no significant endothermic or exothermic peaks were observed in Fig. 2.10(A), one endothermic peak corresponding to aluminum melting was observed near 673^{o}C in Fig. 2.10(B), (C) and (D). Fig.2.10(C) and (D), however, show not only endothermic of aluminum melting, but a strong exothermic peak above 900^{o}C. The exothermic in Fig 2.10(C) corresponds to aluminothermic reduction of TiO_2 while that in Fig. 2.10 (D) corresponds to a sequential reaction of the aluminothermic reduction and TiC synthesis.

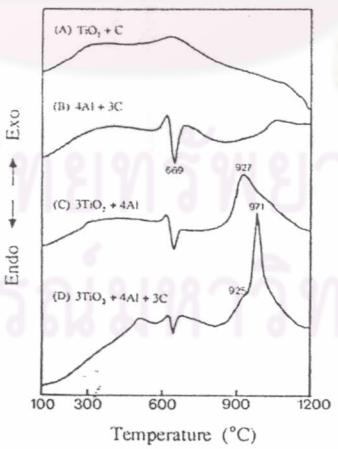

Fig. 2.10 DTA curves of compacted samples with a heating rate of 40^{o}C/min under argon atmosphere [32].

Thus, it is believed, from thermal analysis result, that the reaction is initiated by reaction between titania and aluminum. The sequence of reaction to produce this Al_2O_3-TiC composite is thought to be as below.

(i) The aluminum phase melts and reacts with the titania at 900°C producing titanium and alumina

$$3TiO_2 + 4Al \longrightarrow 3Ti + 2Al_2O_3 \quad (2.4)$$

(ii) The titanium reacts with the free carbon resulting in titanium carbide.

$$Ti + C \longrightarrow TiC \quad (2\text{-}5)$$

Al_2O_3-TiC composites could be sintered pressurelessly during the SHS reaction and have microstructure consisting of layered patterns as shown in Fig. 2.11[32]. The thermal structures in the reaction zone during the combustion were studied. Intermediate Ti or titanium aluminide species, present in aluminothermic reduction of TiO_2 to form Al_2O_3, were not observed in the presence of C, because of the high thermodynamic stability of TiC. The analysis of combustion wave structures confirmed that the wave front propagated in an unstable mode. It was also observed that the combustion products consisted of layered structures with periodicity as shown in fig. 2.11.

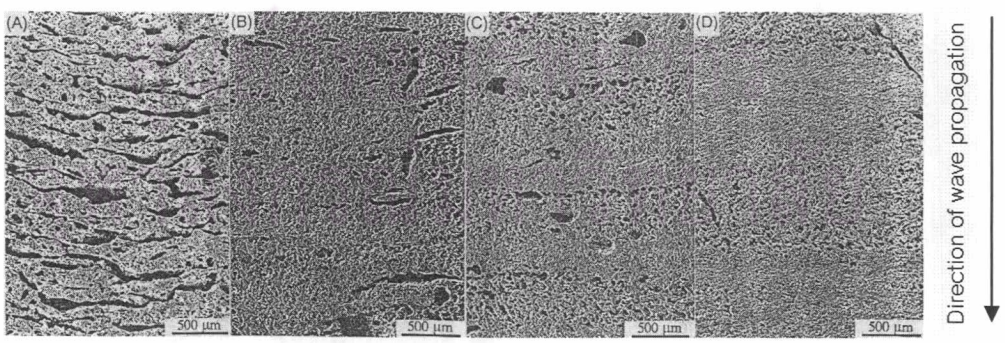

Fig. 2.11 SEM micrographs of polished surface of products combustion synthesized with the addition of (a) 0, (b) 12. (c) 18, (d) 24 wt% Al_2O_3 in $3TiO_2$+4Al+3C sample [32].

2.5.5 Processing Parameters Affect to SHS Characteristic of Al_2O_3-TiC

The effects of a variety of processing parameters have been investigated for SHS reaction of Al_2O_3-TiC composites by C.R.Bowen et al [29]. The microstructure has been shown to be highly dependent on the particle size of each of the reactants. The effect highlights the importance of relative sizes of each particle as this may produce different reactant particle arrangement and result in different microstructure. The study of adding diluents to control the highly exothermic SHS reaction found that use of an Al_2O_3 diluent tends to induce cracking in the final product when the combustion temperature falls below the melting point of alumina phase. As no liquid phase is present during the reaction thermal stresses are not relieved which causes cracking. The use of aluminum as a diluent was suggested because it could be enhanced diffusion process or heat transfer. Preheating has been employed to increase the reaction rate and the combustion wave velocity by increasing the adiabatic combustion temperature of an SHS reaction.

The drawback of the process is that it is extremely violent and energetic leading to less than theoretical density in the product and a low degree of control over the microstructure of product. ZrO_2 nanoparticles were used towards controlling the exothermic reaction [33]. It can be seen in Fig. 2.12 that the combustion synthesized products without ZrO_2 were loosening and there were numerous pores. Sample with 15 wt% ZrO_2 shown less porous pores because the reaction becomes less vigorous with the lower adiabatic temperature.

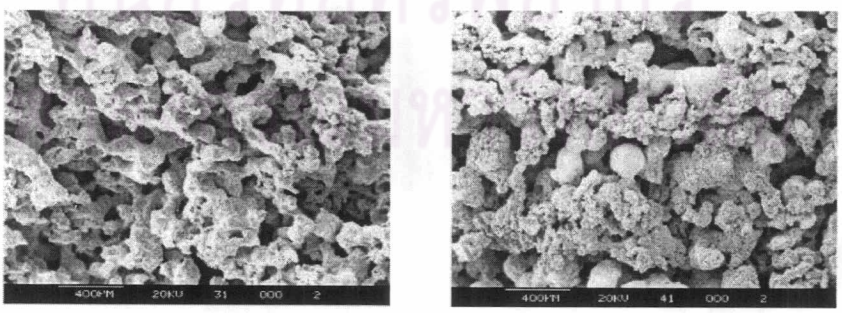

(a) (b)

Fig. 2.12 SEM micrograph of as-combusted (a) Al_2O_3-TiC and (b) Al_2O_3-TiC-15wt. %ZrO_2 Nanocomposite [33].

The thermal explosion method under high pressure or high-pressure self-combustion sintering (HPCS) was carried out to fabricate the dense Al_2O_3-TiC composites in one step [28]. The sample had unique microstructure which was quite different from that of commercial Al_2O_3-TiC materials made by conventional processing. Fig 2.13 shows the fracture toughness value (K_{IC}) as a function of TiC content. The HPCS sample has a high K_{IC} value than commercial sample made by conventional process. This result may reflect the difference in the fracture mode. In the HPCS sample, transgranular fracture in the Al_2O_3 was observed, that was quite different from commercial sample, only intergranular fracture was found.

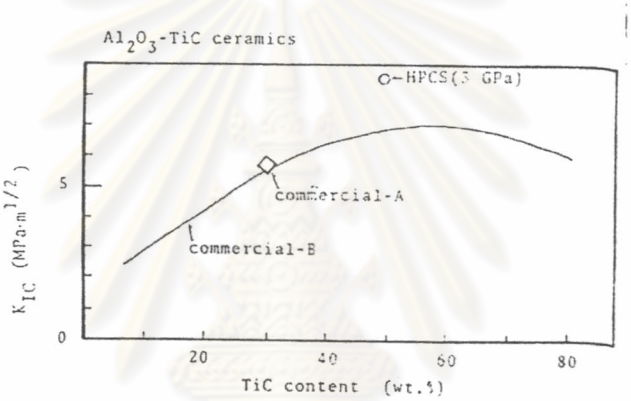

Fig. 2.13 Fracture toughness as a function of TiC content [28].

2.5.6 Effect of Precursors on the Combustion Synthesis of Al_2O_3-TiC

The different types of precursors such as anatase and rutile titania powder, as well as graphite and carbon black powder, were used to investigate the effect on combustion synthesis of Al_2O_3-TiC composites [34]. Fig. 2.14 shows the calculated adiabatic temperature as a function of Al_2O_3 diluent and initial temperature in the combustion system using a different type of TiO_2.

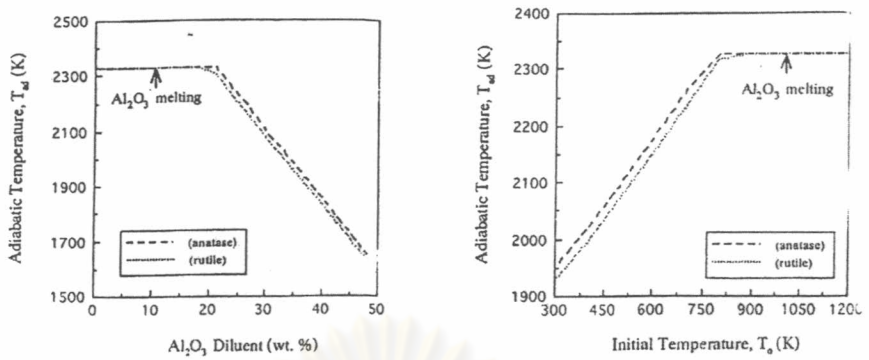

(a) (b)

Fig. 2.14 Calculated adiabatic temperature as a function of (a) the amount of Al_2O_3 diluent and (b) the initial temperature of sample diluted with 36wt. % Al_2O_3 [34].

The results indicate that the exothermicity of sample containing anatase is slightly higher than that rutile. The temperature profile in reaction zone was more dependent on carbon source than titania as was shown in Fig. 2.15. The initial heating rate in graphite system was approximately 6 x 10^3 K/sec and 2 x 10^3 K/sec in the case of carbon black system. Fig. 2.16 shows the structures of the wave front to an axial direction in a given time interval gradually decreased in the order of (a), (b), (c) and (d). Especially, in the case of Fig.2.16 (d), the wave front proceeding in the axial direction was competing with propagation in the radial direction because of its weak exothermicity.

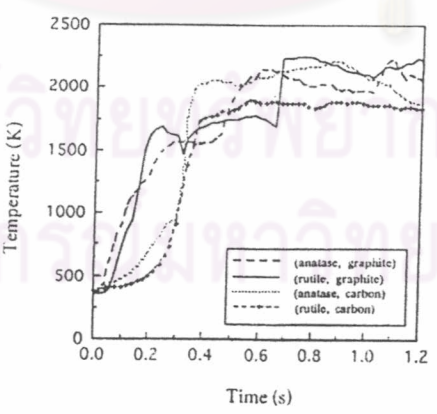

Fig. 2.15 Heating profiles as a function of time in reaction zones during the combustion reaction of $3TiO_2$ + 4Al + 3C sample [34].

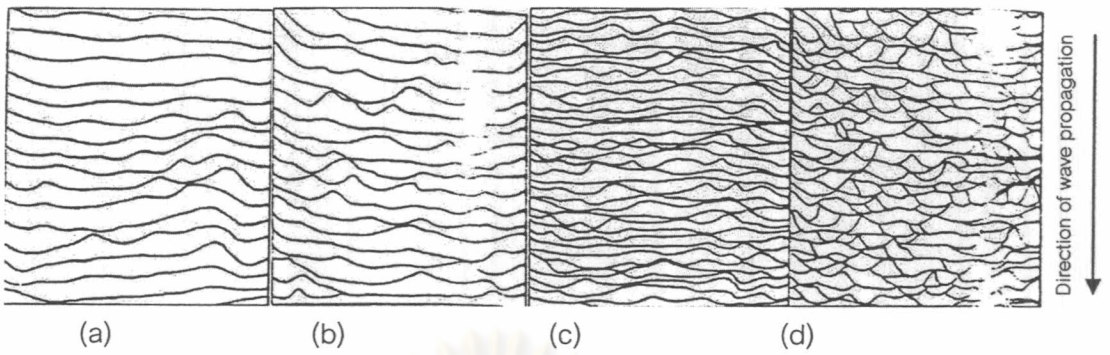

Fig. 2.16 Combustion wave structures in the sample (a) anatase-graphite (b) rutile-graphite (c) anatase-carbon black and (d) rutile-carbon black [34].

The effect of the preheating temperature on the combustion temperature of reaction varying with carbon source was examined [35]. As expected, the combustion temperature and the combustion velocity of reaction increase as the preheating temperature increase. According to the Fig. 2.17, charcoal as carbon source has the highest combustion temperature and velocity of all. The X-ray diffraction patterns and the microstructure of the product were not shown different due to the carbon source.

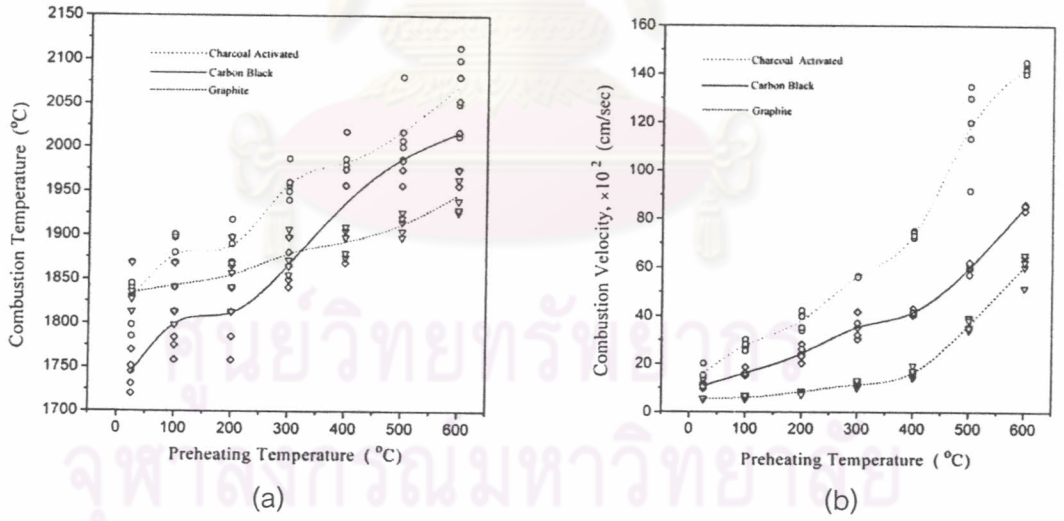

Fig. 2.17 The effect of preheating temperature on (a) combustion temperature and (b) combustion velocity with varying carbon source.

2.5.7 Al_2O_3-TiC Powder Prepared by SHS Process and Sintering Behavior

The goal of many researchers has been to find a way to use the heat generated by the exothermic reaction to supply the high temperature needed for sintering ceramic materials thus allowing a low cost method for densifying advanced ceramic. Primarily because of volume changes between reactant and products, due to volatile gases released during the exothermic excursions, for obtaining densities greater than 98%TD, the one method was using high pressure supplied during the combustion. This was presently no low cost and rapid methods [28]. The high fracture toughness and good strength of the product, however, are the main advantages resulting from this exothermic reaction process.

By controlling the size of reactant, it is possible to make submicrometer ceramic powder using exothermic reaction. These powders can subsequently be pressureless sintered to make dense ceramic. R.A.Cutler et al. [36] prepared Al_2O_3-TiC composite from non-stoichiometric reaction presented in equation (2.6), which could control Al_2O_3-TiC ratio in powder product. The mechanical properties of hot-pressed composites made from SHS powder were comparable to the properties of conventional hot-pressed cutting tools as shown in Table 2.4.

$$3TiO_2 + 4Al + 3C + x\,Al_2O_3 \longrightarrow 3TiC + (2+x)\,Al_2O_3 \qquad (2.6)$$

Table 2.4 Properties of hot-pressed Al_2O_3-TiC composites [36].

Powder method	TiC (wt.%)	Density (g/cm^3)	Strength (MPa)	Hardness (GPa)	Fracture toughness ($MPa.M^{1/2}$)
Conventional	30	4.25	600 - 800	19 -22	3.8 – 4.5
SHS(as-reacted)	30	4.22	666 ± 91	22.1 ± 2.0	3.3 ± 0.3
SHS(milled)	30	4.23	624 ± 208	23.4 ± 1.2	3.7 ±0.1
SHS(as-reacted)	40	4.16	588 ± 114	18.8 ± 1.1	3.9 ±0.3
SHS(milled)	40	4.47	741 ± 83	22.6 ± 1.2	5.5 ±0.4
SHS(milled)	47	4.54	756 ± 185	21.4 ± 0.6	5.7 ±0.2

R.A.Cutler et al. also reported the mechanical properties of pressureless sintered Al_2O_3-30wt.% TiC in comparison to a similar composition sintered with TiH_2 as a densification aid as shown in Table 2.5. The mechanical properties of the pressureless sinter composites made from SHS powder were comparable to or better than the properties of composites sintered using commercial powder.

Table 2.5 Properties of pressureless sintered Al_2O_3-30wt.%TiC composites [36].

Powder method	HIPed	Density (g/cm^3)	Strength (MPa)	Hardness (GPa)	Fracture toughness ($MPa.M^{1/2}$)
SHS	No	4.23	387 ± 80	22.0 ±1.3	4.4 ± 0.3
SHS	Yes	4.25	548 ± 113	22.8 ± 0.9	4.9 ± 0.8
LPA	No	4.03	480 ± 94	18.7 ± 0.6	4.4 ± 0.2
LPA	Yes	4.23	638 ±127	22.0 ± 1.1	4.4 ± 0.5

LPA: Liquid-phase assisted sintering

The combustion reaction characteristics were discussed when activated charcoal, carbon black and graphite were used as carbon source [37]. Fig. 2.18 shows SEM micrograph of SHS product with varying preheating temperature of each carbon source. The products were irregular shape and did not show any significant difference in morphology, however, the particle size of TiC increased with preheating temperature. The combustion temperatures of sample with activated carbon were observed to be higher than other carbon source as shown in Table 2.6.

Table 2.7 shows the physical and mechanical properties of pressureless sintered Al_2O_3-46.8wt%TiC composites with different carbon source. It was found that the overall properties were uniform irrespective of carbon source [37]. In addition, it seen that the SHS Al_2O_3-TiC powder has comparable sintering characteristics to the commercial powder from the result depicted in Table 2.8. Actually the characteristics of pressureless sintered composites were superior in the SHS powder, whereas relatively poor sintering characteristics were observed in the hot-pressed sample. However, the differences are

negligible and it is believed that the SHS process is one of the promising methods of ceramic composite powder production.

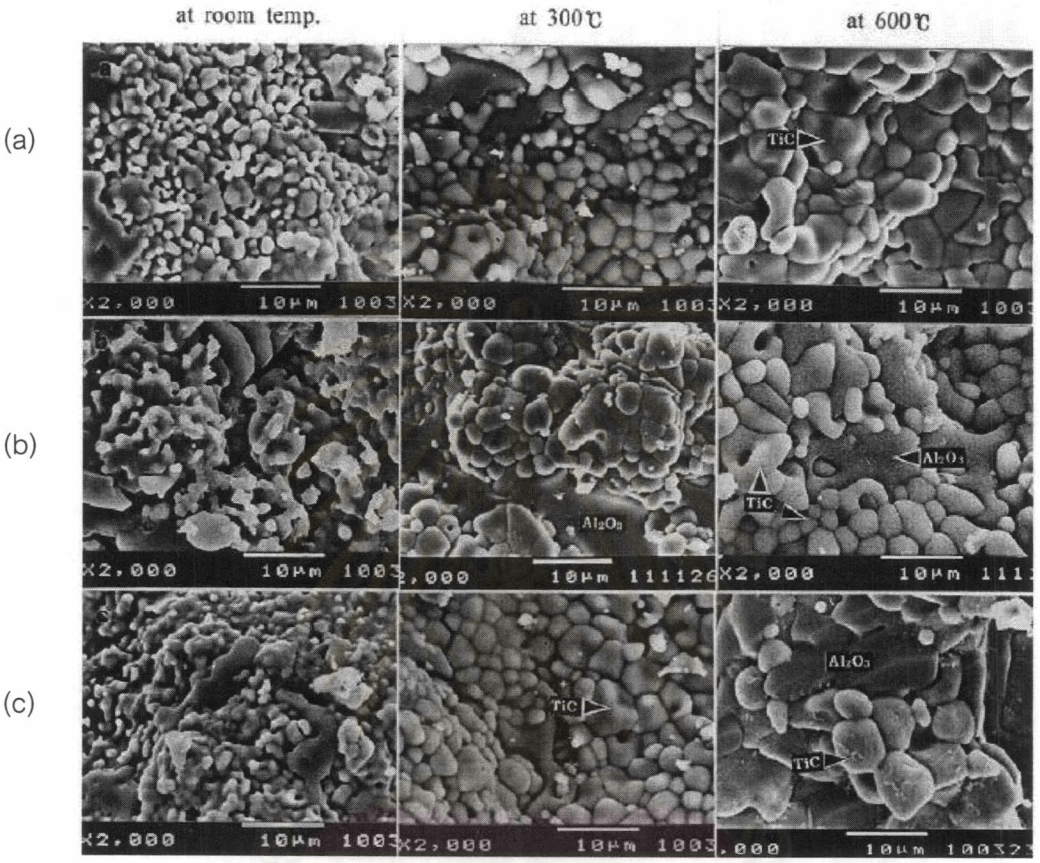

Fig. 2.18 SEM micrographs of SHS products varying with preheating temperature and carbon source:(a) activated carbon (b) carbon black and (c) graphite [37].

Table 2.6 Measured combustion temperatures of the reactants under various preheating temperature and carbon source [37].

Preheating Temp. (^{o}C)	Activated carbon	Carbon black	Graphite
25	1841	1731	1732
300	1957	1841	1869
600	2115	1987	1957

Table 2.7 Properties comparisons of the pressureless sintered Al_2O_3-46.8wt.%TiC composites with variouscarbon sources [37]. (Temperature: 1890^{o}C, time 20 min)

Carbon source	Density (%TD)	Hardness (GPa)	Bending strength (MPa)	Fracture toughness (MPa.M$^{1/2}$)
Activated carbon	95.5	17.4	470 $\pm$ 57	4.3 $\pm$ 0.4
Carbon black	94.8	17.3	460 $\pm$ 64	4.5 $\pm$ 0.4
Graphite	95.2	17.5	468 $\pm$ 43	4.9 $\pm$ 0.2

Table 2.8 Properties of Al_2O_3-46.8wt.%TiC composites prepared by SHS and mixed commercial powder [37].

Sintering Method	Powder method	Density (%TD)	Hardness (GPa)	Bending strength (MPa)	Fracture toughness (MPa.M$^{1/2}$)
Pressureless	SHS	95.2	17.5	468 $\pm$ 43	4.9 $\pm$ 0.2
	Commercial	95.1	16.9	420 $\pm$ 54	5.2 $\pm$ 0.3
Hot-pressing	SHS	98.8	20.5	775 $\pm$ 40	4.2 $\pm$ 0.3
	Commercial	99.2	20.9	810 $\pm$ 70	4.7 $\pm$ 0.4

2.6 Microwave Processing of Ceramics

Microwave are electromagnetic waves that have a frequency range of 0.3 to 300 GHz and corresponding wavelengths ranging from 1 m to 1mm as shown in electromagnetic spectrum in Fig. 2.19. Typical frequency for materials process is 2.45 GHz. It has long been established that a dielectric materials, such as many type of ceramics can be heated with energy in the from of microwaves [5].

In the middle of 1960's, W.R.Tinga and W.A.C.Voss found the feasibility of microwave processing of ceramics, afterwards W.H.Sutton was the first researcher who reported phenomenon that ceramic materials were heated by microwave energy. There are several reasons for the growing interest in microwave processing over conventional processing methods, including the potential for significant reductions in the manufacturing costs due to energy savings and shorter processing time. This process improved product uniformity and yield, provided unique microstructure and properties due to selective heating. Moreover microwave can be used for synthesis a new material as well.

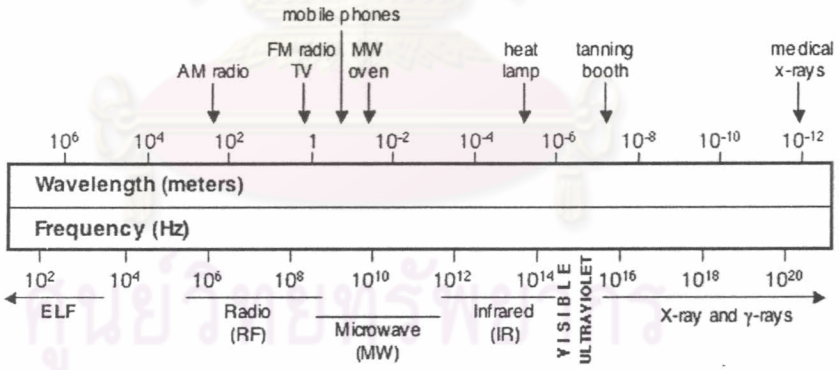

Fig. 2.19 Electromagnetic spectrum

2.6.1 Microwave and materials Interaction

In contrast with visible waves, except for lasers, microwaves are coherent and polarized. Microwaves also obey the law of optics and can be transmitted, absorbed or reflected depending on the material type as illustrated in Fig.2.21.

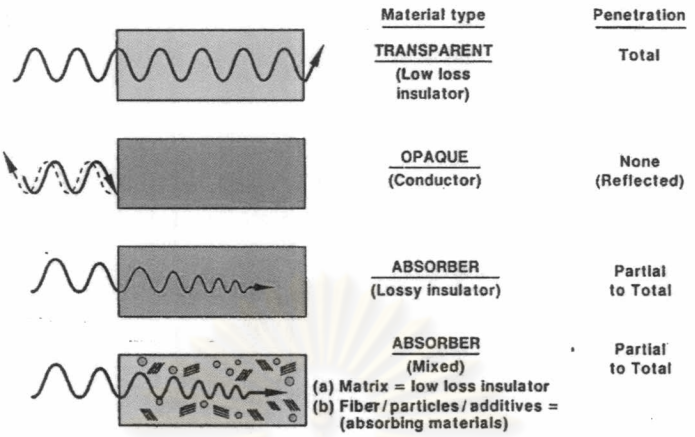

Fig. 2.21 Interaction of microwaves with materials [5].

2.6.1.1 Transparent materials: Microwave can penetrate to these materials such as Al_2O_3, SiO_2, TiO_2, MgO, glass and Pyrex, therefore no heating occurs.

2.6.1.2 Opaque materials: Metals are opaque to microwave and thus are good reflectors, however, microwave will slightly penetrate into surface of very small metal particle and may create surface currents, which leads to surface heating of these materials.

2.6.1.3 Absorber materials: Broad ranges of ceramic dielectric or electrically insulating ceramic are microwaves absorber such as SiC, C, and TiC, which results in microwave heating

2.6.1.4 Mixed absorber materials: In these materials, the microwave absorber materials were added to transparent materials. The heat was conducted from absorber materials to transparent matrix phase, thus the entire sample was heated.

2.6.2 Microwave Heating mechanism

When microwaves penetrate and propagate through a dielectric material, the internal electric field is generated within the affected volume thus induce polarization and motion of charge. The resistance to these induced motions due to material elastic and frictional forces, which are frequentcy dependent, causes losses and attenuates the electric field. As a consequence of these losses, volumetric heating occurs. Microwave heating is

fundamentally different from conventional processes. The reverse temperature gradient was observed in microwave heating as compared to conventional heating as illustrated in Fig. 2.2. The comparison between microwave and conventional process is described in Table 2.9.

Table 2.9 Heating mechanism comparison between conventional and microwave process.

Conventional process	Microwave process
• Radiant heat source : gas burners, electric resistance element • Heat transfer mechanism : - From heat source to surface: convection and radiation - From surface to center: conduction • Surface is at higher temperature than center.	• Microwave sources: Magnetrons, traveling wave tube, 25 transmission lines • Heat generation occurs internally. • Sample is at higher temperature than surrounding. • Heat loss from surface by convection and radiation. • Center is at higher temperature than surface.

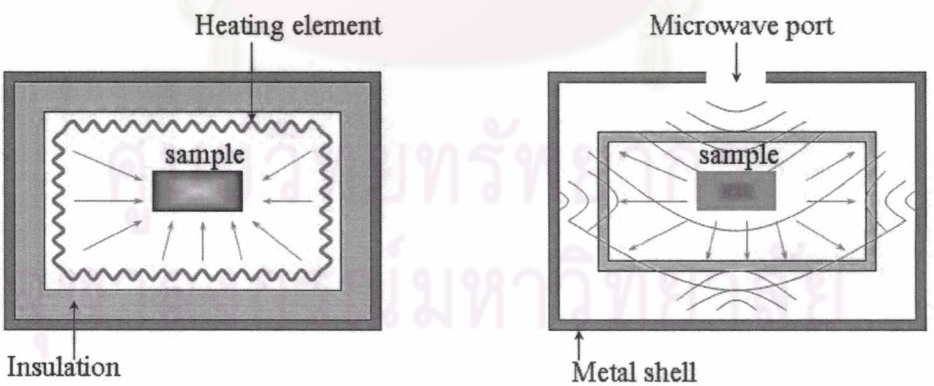

Fig. 2.20 Heating patterns in conventional and microwave furnaces.

2.6.3 Dielectric Loss Mechanism

In the microwave frequency range there are primarily two physical mechanisms through which energy can be transferred to ceramic material.

2.6.3.1 Conduction (Ohmic Conduction): There is a flow of conductive currents, long range motion of charge carrier, resulting in an ohmic type of loss mechanism where the ceramic conductivity(σ) plays a prominent role. The conduction can divide into electronic conduction and ionic conduction. Electronic conduction has an electron as a carrier appears in metal or semiconductor, whereas ionic conduction has ion carriers move and collide with others; occur in ionic material or ceramic. These loss mechanisms are dominated at low frequency, losses decrease with higher frequency due to a decreasing of time allowed for transport in the direction of field.

2.6.3.2 Polarization: At the higher frequency, losses are a result of the dipoles resistances to oscillation and/or rotation under an alternating field as is shown in Fig. 2.22. Four primary mechanisms of polarization are illustrated in Fig. 2.23, electric polarization (P_e), ionic or atomic polarization (P_i), dipole or orientation polarization (P_o) and interfacial or space charge polarization (P_s). The total polarizability of the dielectric can be represented as the sum of these polarizations:

$$P = P_e + P_i + P_o + P_s \tag{2.7}$$

Electronic and ionic polarizations do not generally contribute to microwave absorbtion. These dipole acts as so fast that the net polarization under an electronic field at microwave frequency is in phase with the electronic field, resulting in large restoring forces and small damping effect. Dipole and interfacial polarizations are the most important for microwave heating because they can occur over the frequency range of microwave. As the frequency of electric field increases, the rotation of the dipole can not follow, and the net polarization in the materials is no longer in phase with the electric field. The resistance to dipole is equivalent to large damping effect resulting in relaxation type absorption.

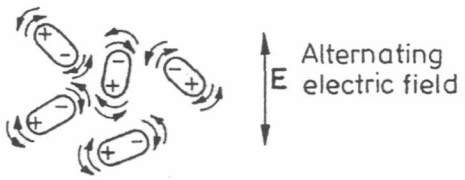

Fig. 2.22 Dipole reorientation with alternating electric field.

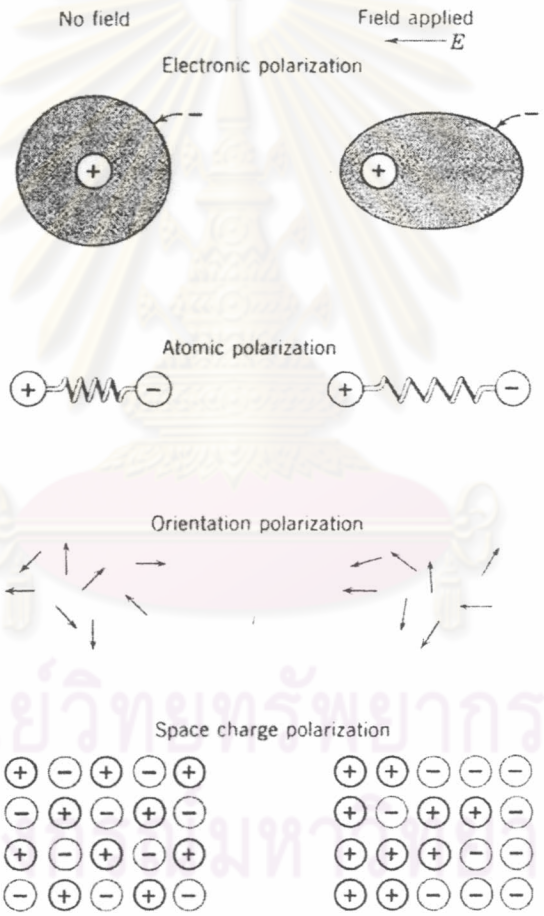

Fig. 2.23 Schematic represents the different mechanisms of polarizations [16].

Polarization is related to the dielectric constant, this relationship can be established by considering dielectric displacement, D, or a quantity of charge per unit area of capacitor plate. Consider dielectric displacement in vacuum.

$$D_o = \varepsilon_o E \tag{2.8}$$

Where

D_o = dielectric in vacuum (C/m^2)

ε_o = permittivity of free space = 8.85×10^{-12} F/m

E = electric field strength (volt/m)

and the dielectric displacement in materials is given by

$$D = \varepsilon' E \tag{2.9}$$

where

ε' = permittivity of materials (F/m)

The permittivity or dielectric constant is often identified as a measurement relative to the permittivity of free space (ε^o). The relative permittivity (ε'_r) is expressed as

$$\varepsilon'_r = \frac{\varepsilon'}{\varepsilon_o} \tag{2.10}$$

In other words, the total dielectric is the sum of dielectric that would have been present in vacuum and an extra charge that results from polarization of dielectric material. Making use of this definition one finds that

$$D = \varepsilon_o E + P \tag{2.11}$$

thus combining equation (2.9), (2.10) and (2.11), obtains

$$\varepsilon' E = \varepsilon_o E + P$$

or

$$\varepsilon'_r \varepsilon_o E = \varepsilon_o E + P \tag{2.12}$$

Thus, equation (2.12) can be rearranged as

$$P=(\varepsilon_r'-1)\varepsilon_o E=\chi\varepsilon_o E \tag{2.13}$$

Where the quantity $(\varepsilon_r'-1)$ is the dielectric susceptibility of material known as χ.

The polarization (P) can also be thought of as the total dipole moment per unit volume of the dielectric materials. A dipole moment, μ, show in Fig. 2.24 is defined as

$$\mu=q\delta \tag{2.14}$$

where

μ = induced dipole moment (C-m)

q = charge (C)

δ = separation distance of positive and negative charge (m)

If there are N dipoles per unit volume (1/m^3), the polarization is then given by

$$P=N\mu=Nq\delta \tag{2.15}$$

Refer to equation (2.13), one sees that

$$P=(\varepsilon_r'-1)\varepsilon_o E=Nq\delta$$

Rearranging this expressing yields

$$\varepsilon_r'-1=\frac{Nq\delta}{\varepsilon_o E} \tag{2.16}$$

This shows that materials properties influencing the dielectric constant include number of dipoles, charge of dipoles and the separation distance between charges.

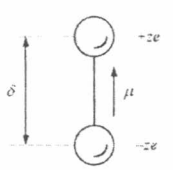

Fig. 2.24 Illustration of an electric dipole moment [10].

The complex interaction of sinusoidal applied voltage with dielectric materials can be illustrated by a vectorial representation of two induced currents namely charging current (I_c) and loss current (I_l) as seen in Fig. 2.25 [10].

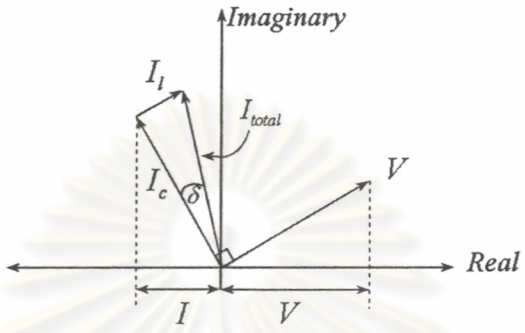

Fig. 2.25 Vectorial representation of applied voltage, loss current and total current dielectric.

In an ideal dielectric, when an alternating voltage is applied across it, an alternating current will flow to and from it due to its charging and discharging successively, which leads the voltage 90°. Total current would be only charging current (I_c). In reality, there is the resistive current (loss current or leakage current), I_l, which is in phase with the applied voltage. Loss current combines with the charging current to give a total current, I_{total}, which leads the applied voltage by an angle 90°-δ, where δ is know as loss angle or loss tangent or dissipation factor.

The loss current arises for two reasons: (1) the direct current conduction losses (I_{dc}) involves the long range motion of charge carrier and (2) dielectric losses (I_{ac}) referred to as alternating conduction losses, results from the dipole resistance to oscillation and /or rotation under an alternating current field.

The concept of charging and losses in an adiabatic can also be expressed by using a material's complex permittivity or dielectric constant (ε^*, F/m) which is composed of a real part and an imaginary part by

$$\varepsilon^* = \varepsilon' - i\varepsilon'' = \varepsilon_o(\varepsilon_r' - i\varepsilon_r'') \tag{2.17}$$

Real part: explain the charging behavior (polarizability) of a material in an electric field.

ε' = dielectric constant or permittivity

ε_r' = relative dielectric constant or relative permittivity

Imaginary part: indicate the materials ability to store the energy.

ε'' = dielectric loss factor

ε_r'' = relative dielectric loss factor

In practice however, the loss tangent or dissipation factor is used to described these losses. It indicates the ability of material to convert absorbed microwave energy into heat and is given by:

$$\tan\delta = \frac{I_i}{I_c} = \frac{\varepsilon_r''}{\varepsilon_r'} = \frac{\sigma}{2\pi f \varepsilon_o \varepsilon_r'} \tag{2.18}$$

where

σ = total effective conductivity (Ω/m)

f = frequency (GHz)

2.6.4 Energy Conversion [38, 39]

The dielectric properties of materials in combination with the applied electromagnetic fields result in the conversion of electromagnetic energy to heat. The power absorbed per unit volume, P_A (W/m^3), provides the following basis of heating:

$$P_A = \frac{P}{V} = 2\pi f \varepsilon_o \varepsilon_r' \tan\delta |E_{rms}|^2 \tag{2.19}$$

where

$$E_{rms} = \frac{E_o}{\sqrt{2}}$$

= root mean square internal electric field (V/m)

E_o = amplitude of electric field (V/m)

Equation (2.19) shows that the power absorbed varies linearly with the frequency, the relative dielectric constant, loss tangent and the square of the electric field. It is assumed that power absorbed by material is uniform throughout the volume and that thermal equilibrium has been achieved. This is rarely the case, in addition the factor f, ε', $\tan\delta$ and E are all interdependent. Furthermore, E is dependent on the size, geometry and location of the material within a microwave cavity and on the design and volume of the cavity. However equation 2.19 provides a useful approximation of power absorption and describes the basis relationship between the four variable factors.

As microwaves penetrate and propagate through an absorbing materials, energy is absorbed, thus the electric field is attenuated as a function of the distance from surface of materials. A useful parameter describing this behavior is D_p, which is the penetration depth at which the incident power is reduced to 1/e (36.8%) of the absorbed power at the surface.

$$D_p = \frac{\lambda_o}{2\pi(2\varepsilon_r')^{1/2}}[(1+(\tan\delta)^2)^{1/2}-1]^{-1/2} \qquad (2.20)$$

where

D_p = depth of penetration

λ_o = incident wavelength

Although low frequencies result in greater λ_o and more penetration depths, the heating does not necessarily increase, since the internal field (E) could be low, depending on the properties of material [5]. If the penetration depth is more than sample dimension, volumetric and uniform heating occur. If the penetration depth is much less than the sample dimension, only the surface is heated. The rest of sample is heated through conduction.

As the microwave energy penetrates into the small metal particle, it attenuates to an extent depending upon the effective loss factor. The inverse of the attenuation constant is defined as skin depth (δ).

$$\delta = \frac{1}{\sqrt{\pi f \mu \sigma_{dc}}} = 0.029\sqrt{\rho \lambda_o} \tag{2.21}$$

Where

μ = magnetic permittivity (H/m)

σ = electrical conductivity (S/m)

ρ = electrical resistivity (Ω.m)

For ceramic material, as in the simple case where the temperature rises at a uniform rate throughout the body of the ceramic, the continuity equation for heating rate gives:

$$\frac{\Delta T}{t} = \frac{\pi f \varepsilon_o \varepsilon_r' \tan\delta |E_o|^2}{\rho C_p} \tag{2.22}$$

where

E_o = amplitude of electric field (V/m)

ρ = density (kg/m^3)

C_p = specific heat of material (J.kg^{-1}.^{O}C^{-1})

The relative dielectric constant (ε_r') and loss tangent ($\tan\delta$) are the two most widely used and measure parameters that describe the behavior of a dielectric material under the influence of a microwave field. They both affect the power absorbed (equation 2.19), the depth of penetration (equation 2.20) and heating rate (equation 2.22), thus they influence the volumetric heating behavior of a given material. The value of ε_r' is a measure of polarizability of a material in an electric field, where the value of $\tan\delta$ is a measure of loss (or absorbtion) of microwave energy within the materials

2.6.5 Temperature Effect

During heating ε_r' and $\tan\delta$ change with temperature, and a knowledge of these changes is important for process control. Fig 2.26 shows that ε_r of various materials increase slowly from room temperature to 1400°C and that ε_r' of Al_2O_3 increases at a greater rate. The increase in ε_r' with temperature is due to an increase in the polarizability caused by volumetric expansion.

In contrast to ε_r', $\tan\delta$ is far more affected by temperature, as shown Fig. 2.27. In general, $\tan\delta$ initially rises slowly with increasing temperature, until some critical point (T_{crit}) is reached, beyond with $\tan\delta$ rises rapidly. Compositional additives and impurities usually account for the rapid rise in $\tan\delta$ in polycrystalline ceramics is associated with the softening of intergranular, amorphous phase, which causes an increase in the local conductivity in equation 2.18. This could explain situation in Fig. 2.27, why $\tan\delta$ of 99% pure alumina sample was less affected by temperature than that of the 97% pure alumina.

At temperature above T_{crit}, $\tan\delta$ rises very rapidly, this causes a condition of thermal runaway in a microwave heated materials. As $\tan\delta$ begins to absorb microwave energy more efficiently, which also raises the temperature, this cause $\tan\delta$ begins to rise even faster. The net results are an exponential increase (runaway) in the temperature. The rate of temperature rise and triggering temperature (T_{crit}) vary widely for different materials.

Thermal runaway is an important aspect of microwave heating; it can cause undesirable hot spots within a material, it can also be used to heat materials at rapid rate. There are several mean to control or prevent thermal runaway such as by controlling or pulsing the microwave power level, where charges in the power cause an instantaneous response in the material. Another method is by designing the microwave system and applicator to deposit the microwave energy within the material or product in a prescribed manner.

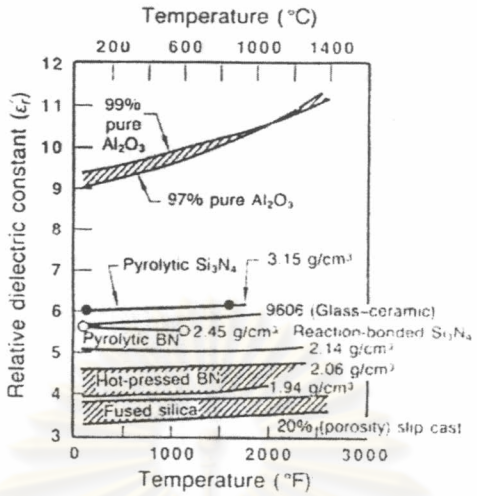

Fig. 2.26 Relative dielectric constant (8 to 10 GHz) versus temperature [5].

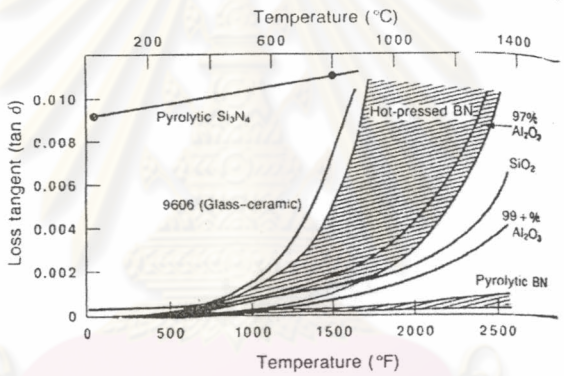

Fig. 2.27 Loss tangent (8 to 10 GHz) versus temperature [5].

2.6.6 Synthesize and Sintering Al_2O_3-TiC by Microwave Energy

Recent publications have reported the use of microwave energy to synthesize ceramic powders where reactions of component oxides at elevated temperature are involved and, in some case, where the influence of the atmosphere is considered [8]. Heat generated by microwave energy depends on the microwave absorbtion efficiency of materials. This, in turn, depends on the dielectric loss factor of material. Therefore, the investigation of combustion synthesis by microwave is more limited attention. However, the use of microwave energy combined with combustion reaction to synthesize Al_2O_3-TiC

powder, received from equation (2.3), was conceivable due to carbon, a precursor in reaction, is high dielectric permittivity material.

A surprising feature of the work by Y.L.Tian et al [40] is that despite the use of an applicator designed to maximize temperature uniformity, severe temperature gradients were found both radially and axially. The sintering of Al_2O_3-30%TiC composites was performed under nitrogen gas pressure of about 1MPa in microwave field. Composite rods were rapidly and uniformly heated to 1850°C and were sintered to 95%TD without cracking. Fig2.28 shows the temperature dependence of density for microwave sintered and conventionally fast-fired Al_2O_3-30%TiC composites. The highest density achieved was 93.2% at 1750°C. This temperature was significantly lower than that required in conventional sintering at the same density (about 1880°C).

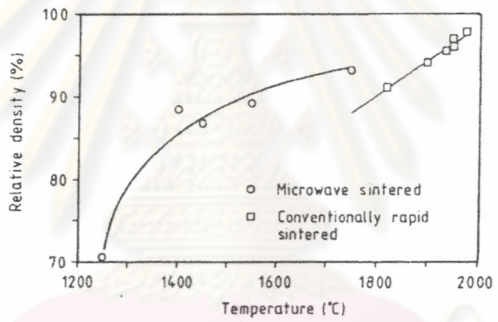

Fig.2.28 Temperature dependence of density for microwave sintered and conventionally fast sintered Al_2O_3-30%TiC [40].

The feasibility of producing Al_2O_3-TiC cutting tools by fast microwave sintering followed by HIP was examined by A.Golstein and A.Singurindi [41]. The density and hardness of the as-sintered specimens show in Table 2.10. The physical and mechanical properties were somewhat lower than required for practical use, but after HIP, acceptable levels of these characteristics were obtained. The use of a particulate SiC susceptor of suitable architecture reduces the fraction of cracked tools in multi-specimen batches.

Table 2.10 Bulk density and mechanical properties of sintered and HIP Al_2O_3-30%TiC ceramic parts.

Sintering conditions		Bulk density (%TD)	H_v (kg/mm^2)	Bulk density (%TD)	H_v (HIP) (kg/mm^2)	K_{IC}(HIP) ($MPa.m^{1/2}$)
Temp (^oC)	Dwell time (min)					
S1800	15	97.0	1860	98.4	2050	4.32
D1800	15	96.0	1830	98.2	2010	4.38
D1700	20	93.0	1740	-	-	-
D1650	25	89.0	-	-	-	-
Commercial tool		-	-	-	2200	4.80

TD=4.28g/cm^2 for Al_2O_3-30%TiC. D= direct MW heating S= susceptor (SiC) assisted MW heating

In summary, literature review reveals that they have been a few studies on microwave-induced combustion synthesis of Al_2O_3-TiC [8]. Especially, the effect of various types of precursor on ignition behavior under microwave energy has never been carried out. Therefore, it is the purpose of this research to investigate the effect of various types of precursors on microwave combustion behavior and powder characteristics of Al_2O_3-47wt%TiC powders and also compare with conventional synthesis system. Moreover the preliminary of microwave sintering was examined.